Issue 28, 2020

Previous Article | Next Article

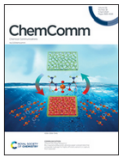

From the journal:
Chemical Communications

In situ catalyst reactivation for enhancing alcohol electro-oxidation and coupled hydrogen generation†

Daniel Martín-Yerga, ‡*[a] Xiaowen Yu,[b] Irina Terekhina,[b] Gunnar Henriksson[c] and Ann Cornell*[a]

COMMUNICATION

In situ catalyst reactivation for enhancing alcohol electro-oxidation and coupled hydrogen generation

Received 00th January 20xx,
Accepted 00th January 20xx

DOI: 10.1039/x0xx00000x

Daniel Martín-Yerga[a*#], Xiaowen Yu[b], Irina Terekhina[b], Gunnar Henriksson[c] and Ann Cornell[a*]

A novel method exploiting the in situ reactivation of a PdNi catalyst to enhance the electro-oxidation of alcohols is reported. The periodic regeneration of the catalyst surface leads to significant gains in terms of conversion rate, energy requirements and stability compared to the conventional potentiostatic method.

Clean processes for the sustainable generation of energy, fuels and platform chemicals are urgently needed in order to replace those based on fossil-based feedstocks with the ultimate goal of protecting the environment. In this regard, electrochemistry is well-placed as a viable option towards green chemical processes since electrons are the main reactant, limiting the use of toxic reagents or solvents, and mild conditions are typically employed.[1,2] For instance, electrochemical oxidation of alcohols such as methanol, ethanol or glycerol can lead to the production of value-added chemicals from sustainable biomass sources, and thus, has attracted significant attention in the last years.[3–5] Coupled generation of hydrogen at the cathode is possible leading to the simultaneous production of valuable chemicals and a clean fuel.[6–8]

Cyclic voltammetry is a fundamental tool to evaluate the electrocatalytic performance of alcohol oxidation. Noble metal catalysts have been widely used for this purpose since the potential required to oxidize the alcohol is significantly lower than when using earth-abundant catalysts.[9,10] **Figure 1** shows, schematically, a characteristic cyclic voltammetry for alcohol oxidation using noble metal-based catalysts, where two different anodic peaks are observed during the forward and backward potential sweeps.[11,12] Fundamental insights about the catalyst and reaction intermediates have been interpreted from the ratio between the forward and backward anodic peak current densities (j_{pf}/j_{pb}). For instance, this ratio was historically used to describe the tolerance of the catalyst to poisoning by carbonaceous intermediates formed during the forward sweep,[13] and this interpretation has been widely used.[14–16] In this context, a high j_{pf}/j_{pb} ratio was taken as the ability of the catalyst to remove these poisoning species (leading to complete oxidation in the forward sweep). In contrast, a high j_{pb}/j_{pf} ratio would suggest a low-performance catalyst easily blocked by these intermediates. However, several recent studies have challenged this interpretation and assigned the backward anodic process mainly to the oxidation of new alcohol molecules after the catalyst has been reactivated.[11,12] This happens since at higher potentials during the forward sweep, the catalyst becomes deactivated by oxide formation,[17] but the surface is recovered during the backward sweep by reduction of metal oxides[18] leading to the generation of a fresh catalyst surface. The magnitude of this reactivation process (i.e. j_{pb}) may depend on several variables such as the catalyst employed, the specific alcohol reaction and conditions, but a high j_{pb}/j_{pf} ratio would generally suggest a higher activity for the fresh catalyst surface. The standard method for practical electro-oxidation of alcohols has been using the process observed in the forward sweep, i.e. recording/applying potentials near the j_{pf}.

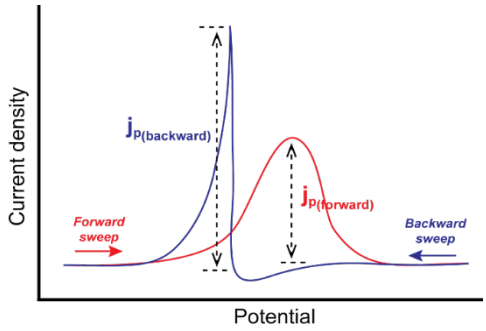

Figure 1. Scheme of a characteristic cyclic voltammetry for alcohol oxidation with noble metal electrocatalysts.

[a] Department of Chemical Engineering, KTH Royal Institute of Technology, SE-10044 Stockholm, Sweden.
[b] Department of Materials and Environmental Chemistry, Stockholm University, SE-10691 Stockholm, Sweden
[c] Department of Fibre and Polymer Technology, KTH Royal Institute of Technology, SE-10044 Stockholm, Sweden.
[#] Current address: Department of Chemistry, University of Warwick, Coventry CV47AL, United Kingdom
*E-mails: daniel.martin-yerga@warwick.ac.uk (D.M-Y); amco@kth.se (A.C)
Electronic Supplementary Information (ESI) available: experimental details, catalyst characterization and additional electrochemical experiments. See DOI: 10.1039/x0xx00000x

However, in cases where the j_{pb}/j_{pf} ratio is significantly high, the electro-oxidation of alcohols after the catalyst reactivation could lead to enhanced performance: higher current densities (i.e. conversion rate) and lower potentials (i.e. energy requirements). However, as far as we are aware, this in situ reactivation process has not been exploited as the foundation for practical alcohol electro-oxidation.

In this work, a novel method to enhance the electro-oxidation of alcohols in terms of higher current density and lower oxidation potential is reported. This is possible by the periodic in situ reactivation of the catalyst to generate a fresh and highly-active surface. As a proof-of-concept, a PdNi catalyst and lactic acid oxidation were employed since high potentials are typically required to oxidize lactic acid at a significant rate, [19–21] but it is a promising sustainable platform chemical.[22,23] PdNi was chosen since bimetallic catalysts have been reported to be more active for alcohol oxidation than monometallic ones due to factors such as the bifunctional mechanism, which describes that the oxophilic metal (Ni) is also involved in the reaction.[24] The proposed method could also be potentially extended to other alcohol-based reactions or catalysts, particularly when the j_{pb}/j_{pf} ratio is well above unity. Furthermore, clean hydrogen fuel is co-produced at the cathode, a reaction which also gets indirectly enhanced by the better performance of the anodic reaction.

Lactic acid (LA) electro-oxidation was studied in alkaline media (NaOH) using a PdNi catalyst electrodeposited on Ni foam (see Supporting Information and **Figures S1-S4** for preparation and characterization details). The presence of Pd as catalyst enables the LA oxidation at low potentials as shown in the cyclic voltammograms for 1 M LA in 1 M NaOH using the PdNi catalyst or bare Ni foam (**Figure 2a**). This suggests that Pd atoms are the active sites for the LA oxidation reaction. **Figure 2b** shows the voltammetric response obtained for increasing LA concentrations, which confirms that the significant anodic processes can be assigned to LA oxidation, since the peak currents increased with concentration. Blank solution (1 M NaOH) shows the typical surface electrochemistry of Pd-based catalysts (see **Figure S5**). These Pd-based surface processes can affect the LA oxidation. Formation of Pd oxides typically deactivates the catalyst surface for alcohol oxidation,[17,25] but the electro-reduction of the oxide layer leads to catalyst reactivation[12,18] and enables LA electro-oxidation during the backward voltammetric sweep. The latter can be recognized by the appearance of a sharp anodic peak around -0.20 V, which coincides with the oxide reduction process as shown in Figure 2b. The j_{pb}/j_{pf} ratio is significantly above unity for the LA oxidation at different concentrations using the PdNi catalyst. Interestingly, even for low LA concentrations (0.05 M), where it is difficult to differentiate the anodic response from that obtained with the blank solution (see blue and red curves in Figure 2b), a significant peak can be observed during the backward sweep, which suggests that the catalyst is more active when in situ regeneration of its surface takes place. While this catalyst response (high j_{pb}/j_{pf} ratio) could be taken as a low-performance catalyst if following the historical interpretation of the j_{pb}/j_{pf} ratio, this work will demonstrate (*vide infra*) that the alcohol oxidation can be significantly enhanced by exploiting the in situ catalyst regeneration.

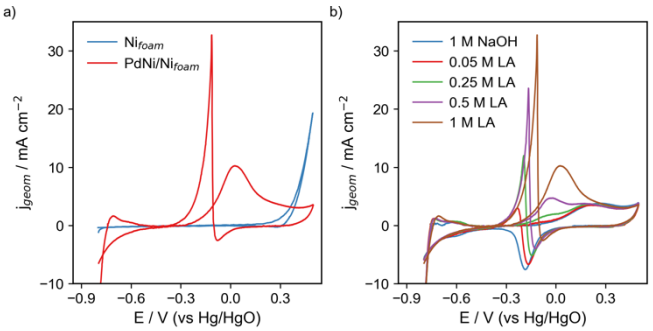

Figure 2. a) Cyclic voltammetry recorded for the oxidation of 1 M LA in 1 M NaOH using the $PdNi/Ni_{foam}$ catalyst (red curve) and bare Ni_{foam} (blue curve) b) Cyclic voltammetries recorded for increasing concentrations of LA (0, 0.05, 0.25, 0.5 and 1 M) in 1 M NaOH using the $PdNi/Ni_{foam}$ catalyst. Scan rate was 10 mV s^{-1} in all cases.

Figure 3a shows the potentiostatic response obtained for the oxidation of 1 M LA in 1 M NaOH at different constant potentials. For the sake of clarity when comparing methods, this method is called conventional method thereafter. The optimal potential for producing the LA oxidation by conventional potentiostatic method was 0 V. A slightly higher current density is initially recorded at +0.05 V, but it decreased more quickly than at 0 V. Since the solution was stirred and no mass transfer limitations should be present under these conditions, the quick current decrease is indicative of catalyst deactivation probably by a higher rate of oxide formation (oxide formation happens at potentials very close to LA oxidation), the oxide layer being inactive for alcohol oxidation.[17]

In order to induce the LA oxidation by a fresh, regenerated catalyst surface, a pulsed potential program was applied. **Figure 3b** shows the current response obtained after applying an initial high potential (E_{high}) of +0.50 V for 5 s, and a low potential (E_{low}) between -0.10 and -0.22 V for 60 s. This pulsed potential program is able to trigger a cascade of electrochemical reactions: at E_{high} the formation of inactive PdO on the catalyst surface takes place, and then at E_{low} the catalyst is in situ regenerated by reduction of PdO to fresh Pd, which enables again the LA electro-oxidation. E_{low} was chosen to be near the potential of the backward anodic peak observed in the voltammograms. A scheme of this in situ reactivation process is shown in **Figure 3c**. The current densities recorded using this method were generally larger and kept higher values for longer times than those obtained by the conventional potentiostatic method, even if the applied potential during LA oxidation (E_{low}) is much lower in this case. Figure 3b also shows a short "dead time" where the current is negative, which depends on the applied potential (E_{low}). This fact is a consequence of a lower rate of PdO reduction when the applied E_{low} are more positive leading to a slower formation of the fresh Pd surface. As a result, the LA oxidation starts at longer times during the experiment. In order to optimize this dead time and enhance the rate of catalyst regeneration, an optimized pulse potential program was selected (**Figure S6**), consisting of applying a E_{high} of +0.6 V for just 100 ms, and then a E_{low} of -0.20 V for 30 s to produce the catalyst regeneration and LA oxidation. A similar issue with

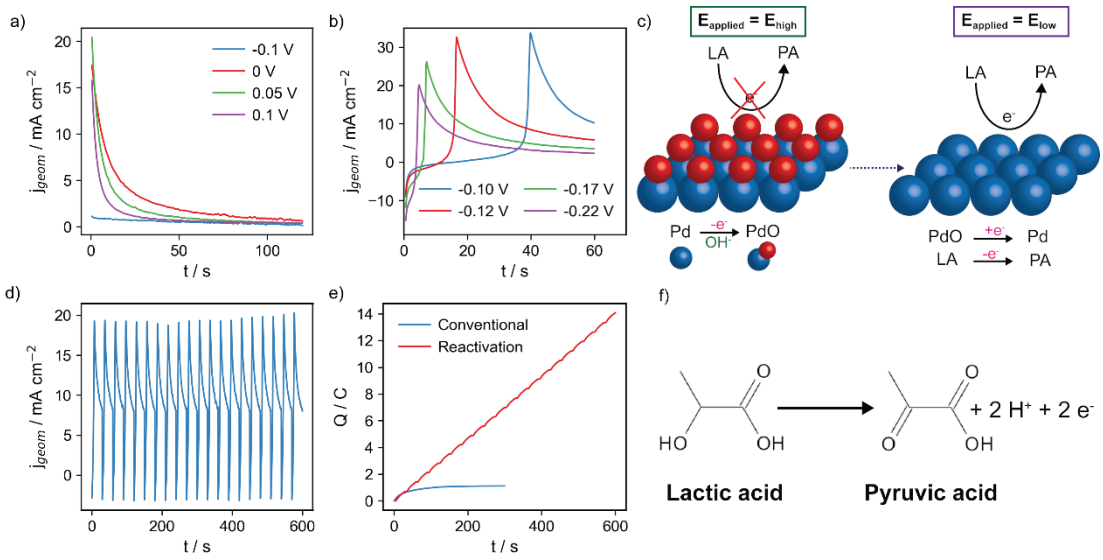

Figure 3. a) Potentiostatic response for the oxidation of 1 M LA in 1 M NaOH at different constant potentials (-0.1, 0, 0.05 and 0.1 V). b) Potentiostatic response for the oxidation of 1 M LA in 1 M NaOH after applying a pulse program consisting of +0.6 V for 5 s and different potentials (-0.10, -0.12, -0.17 and -0.20 V) for 60 s. The response shown is only for the second part of the pulse program (E_{low}). c) Scheme illustrating the catalyst in situ reactivation by applying the potential pulse program (E_{high} and E_{low}). d) Potentiostatic response obtained for the oxidation of 1 M LA in 1 M NaOH by periodic in situ catalyst regeneration (20 pulses of +0.6 V (E_{high}) for 100 ms and -0.20 V (E_{low}) for 30 s). The response shown is only for the second part of the pulse program (E_{low}). e) Accumulated charge recorded for the oxidation of 1 M LA in 1 M NaOH using both methods (conventional and in situ reactivation). f) Scheme for the oxidation of lactic acid to pyruvic acid. All potential values are referred to the Hg/HgO reference electrode.

both methods was the quick decrease of the current densities. Since this deactivation is probably coming from the generation of inactive surface oxides, repetition of the pulse program could be able to periodically regenerate the catalyst surface and maintain a higher conversion rate for longer times. **Figure 3d** shows the response obtained when the optimized pulse program was repeated 20 times (10 min). The initial current response was recorded with good reproducibility throughout the whole experiment, demonstrating that the initial high-activity state of the catalyst can be easily recovered by periodically repeating the pulses. This experimental response also indicates that the deactivation observed during one cycle comes from oxide formation that can be removed by applying E_{low} to regenerate the catalyst surface. In order to confirm that the enhanced response comes by the catalyst regeneration at low potentials and is not a consequence of the pulse program by itself, a pulse at E_{high} was applied between two conventional potentiostatic runs. This experiment consisted in applying: 1) 0 V for 30 s, 2) +0.6 V for 100 ms, and 3) 0 V for 30 s. **Figure S7** shows that the catalyst becomes practically deactivated (currents near zero) after the application of the E_{high} pulse since 0 V is not enough to induce the catalyst reactivation, indicating once more that oxide formation (facilitated at high potentials) induces the catalyst deactivation.

A more convincing way to illustrate the performance of LA oxidation using both methods (conventional and in situ reactivation) is by recording the accumulated transferred charge in function of time during the experiment (**Figure 3e**). For the conventional method, the current densities were smaller (and continuously decreasing) leading to a plateau of accumulated charge after ~200 s when the catalyst was almost completely deactivated (**Figure S8**). In contrast, the accumulated charge for the reactivation method was increasing steadily with the time of experiment as a result of the periodic catalyst regeneration. For instance, the accumulated charge transferred after 300 s was 7 and 1.1 C for the regeneration and conventional methods, respectively (> 500% increment), and it is evident that the difference would be much higher at longer times. The in situ periodic reactivation of the catalyst also shows good performance for much longer experiments with just a slight decrease of the charge transferred after 300 pulses (**Figure S9**), but still with a significant charge transferred for LA oxidation. This demonstrates the good stability of the catalyst using this method in contrast to the conventional method, where catalyst deactivation is observed. In addition, the in situ regeneration method can also be successfully applied to the oxidation of other alcohols such as ethanol (see **Figure S10**).

To evaluate the conversion efficiency for the anodic (LA oxidation) and cathodic (H_2 evolution) reactions using the in situ reactivation method, the amount of products generated were measured. Hydrogen was measured using a gas displacement method where the tubing was connected to the cathodic compartment of a divided cell (with 1 M NaOH). **Figure 4a** shows the volume of H_2 produced at increasing times (accumulated charge) together with the theoretical value expected by Faraday's law, demonstrating an efficiency close to 100% for H_2 production, as expected in a divided cell with only 1 M NaOH in the cathodic compartment. LA oxidation products were analyzed by High-Performance Liquid Chromatography (HPLC). A typical chromatogram is shown in **Figure S11**, where mainly the presence of LA and pyruvic acid (PA) was observed with low signals for other products. A conversion of 3% LA was calculated by quantification of LA before and after the oxidation of 1 M LA for 4h (480 pulses). It is worth to comment that the conversion could be enhanced by using larger-scale electrodes or multi-stack cells as used in industry applications. The product

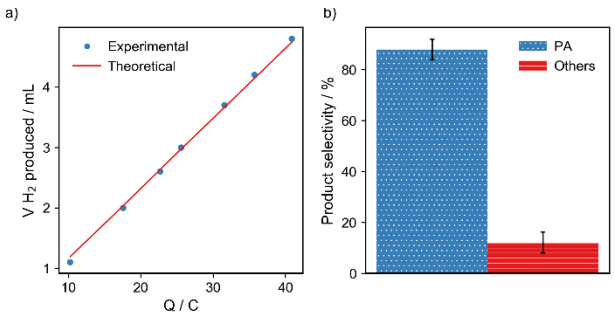

Figure 4. a) Volume of H_2 produced at increasing accumulated charges for the oxidation of 1 M LA in 1 M NaOH using the in situ reactivation method. The cathodic compartment was filled with only 1 M NaOH solution. b) Product distribution obtained by HPLC analysis after oxidation of 1 M LA in 1 M NaOH using the in situ reactivation method

distribution obtained is illustrated in **Figure 4b**, with most of the LA converted to PA (88% selectivity). Therefore, the LA oxidation by in situ catalyst reactivation seems to be very selective for PA production, which entails the transfer of 2 e^- and oxidation of the hydroxyl group of the LA molecule (**Figure 3f**). A high faradaic efficiency was also calculated for the PA formation (81%), demonstrating that most of the applied charge is used for this reaction. The electro-oxidation of LA to products of higher oxidation state has also been reported,[26,27] probably by a subsequent oxidation of PA. However, the in situ reactivation method requires a very low potential for the LA oxidation, while PA oxidation happens at a more positive potential (**Figure S12**) and the catalyst seems to be less active for this reaction. It is particularly interesting to mention that a reactivation process in the backward sweep was not observed for PA oxidation probably because the onset potential for PA oxidation is more positive than the potential where PdO reduction occurs, so when fresh Pd is generated, the applied potential is not high enough to oxidize PA at a significant rate. Therefore, the method reported herein has an intrinsic high selectivity for LA oxidation to PA, and becomes a promising and greener alternative to the standard PA synthetic route by dehydration/decarboxylation of tartaric acid,[28] which requires a considerable amount of energy and stoichiometric amounts of $KHSO_4$.

In conclusion, a novel method to enhance the LA electro-oxidation by in situ catalyst reactivation has been demonstrated with co-generation of valuable products such as PA and H_2. This method shows a higher performance than a conventional potentiostatic method in terms of conversion rate (transferred charge by unit of time), energy requirements (lower potential) and higher catalyst stability (by periodic catalyst regeneration). The possibilities for H_2 production from alcohols containing carboxylic acids seem therefore good. Results reported herein also highlight the importance of not quickly discarding a catalyst showing a low j_{pf}/j_{pb} ratio during initial exploratory voltammetric experiments for alcohol oxidation.

Conflicts of interest

There are no conflicts to declare.

Acknowledgements

We gratefully acknowledge support from the Swedish Energy Agency (Project 44666-1).

Notes and references

1 1 M. Yan, Y. Kawamata and P. S. Baran, *Angew. Chem. Int. Ed.*, 2018, **57**, 4149–4155.
2 2 A. Shatskiy, H. Lundberg and M. D. Kärkäs, *ChemElectroChem*, 2019, **6**, 4067–4092.
3 3 M. S. E. Houache, K. Hughes, A. Ahmed, R. Safari, H. Liu, G. A. Botton and E. A. Baranova, *ACS Sustainable Chem. Eng.*, 2019, acssuschemeng.9b01070.
4 4 X.-Y. Ma, Y. Chen, H. Wang, Q.-X. Li, W.-F. Lin and W.-B. Cai, *Chem. Commun.*, 2018, **54**, 2562–2565.
5 5 M. C. Figueiredo, A. Santasalo-Aarnio, F. J. Vidal-Iglesias, J. Solla-Gullón, J. M. Feliu, K. Kontturi and T. Kallio, *Applied Catalysis B: Environmental*, 2013, **140–141**, 378–385.
6 6 Y. X. Chen, A. Lavacchi, H. A. Miller, M. Bevilacqua, J. Filippi, M. Innocenti, A. Marchionni, W. Oberhauser, L. Wang and F. Vizza, *Nat Commun*, 2014, **5**, 4036.
7 7 B. You, G. Han and Y. Sun, *Chem. Commun.*, 2018, **54**, 5943–5955.
8 8 L. M. Reid, T. Li, Y. Cao and C. P. Berlinguette, *Sustainable Energy Fuels*, 2018, **2**, 1905–1927.
9 9 G. G. W. Lee, J. Leddy and S. D. Minteer, *Chem. Commun.*, 2012, **48**, 11972.
10 10 D. Martín-Yerga, G. Henriksson and A. Cornell, *Electrocatalysis*, 2019, **10**, 489–498.
11 11 D. Y. Chung, K.-J. Lee and Y.-E. Sung, *J. Phys. Chem. C*, 2016, **120**, 9028–9035.
12 12 Y. Zhao, X. Li, J. M. Schechter and Y. Yang, *RSC Adv.*, 2016, **6**, 5384–5390.
13 13 R. Mancharan and J. B. Goodenough, *J. Mater. Chem.*, 1992, **2**, 875.
14 14 T. Nitaya, Y. Cheng, S. Lu, K. Poochinda, K. Pruksathorn and S. P. Jiang, *Chem. Commun.*, 2018, **54**, 12404–12407.
15 15 M. S. Ahmed and S. Jeon, *ACS Catal.*, 2014, **4**, 1830–1837.
16 16 C. Zhu, B. Lan, R.-L. Wei, C.-N. Wang and Y.-Y. Yang, *ACS Catal.*, 2019, **9**, 4046–4053.
17 17 L. Wang, A. Lavacchi, M. Bellini, F. D'Acapito, F. D. Benedetto, M. Innocenti, H. A. Miller, G. Montegrossi, C. Zafferoni and F. Vizza, *Electrochimica Acta*, 2015, **177**, 100–106.
18 18 R. Rahul, R. K. Singh, B. Bera, R. Devivaraprasad and M. Neergat, *Phys. Chem. Chem. Phys.*, 2015, **17**, 15146–15155.
19 19 Z. Xixi, P. Qian and B. Wang, *Appl Microbiol Biotechnol*, 2019, **103**, 4045–4052.
20 20 G. C. Sedenho, P. T. Lee, H. S. Toh, C. Salter, C. Johnston, N. R. Stradiotto and R. G. Compton, *Int. J. Electrochem. Sci.*, 2016, **11**, 11.
21 21 G. Horányi, *Journal of Electroanalytical Chemistry and Interfacial Electrochemistry*, 1981, **117**, 131–137.
22 22 A. Corma, S. Iborra and A. Velty, *Chem. Rev.*, 2007, **107**, 2411–2502.
23 23 J. J. Bozell and G. R. Petersen, *Green Chem.*, 2010, **12**, 539.
24 24 C. Shang and E. Wang, *Phys. Chem. Chem. Phys.*, 2019, **21**, 21185–21199.
25 25 P. V. B. Santiago, R. A. G. Oliveira, J. M. Roquetto, N. Akiba, I. Gaubeur, C. A. Angelucci, J. Souza-Garcia and J. M. Feliu, *Electrochimica Acta*, 2019, **317**, 694–700.
26 26 A. Yuksel, M. Sasaki and M. Goto, *Ind. Eng. Chem. Res.*, 2011, **50**, 728–734.
27 27 C. Chen, A. J. Bloomfield and S. W. Sheehan, *Ind. Eng. Chem. Res.*, 2017, **56**, 3560–3567.
28 P. Xu, J. Qiu, C. Gao and C. Ma, *Journal of Bioscience and Bioengineering*, 2008, **105**, 169–175.

SUPPORTING INFORMATION

In situ catalyst reactivation for enhancing alcohol electro-oxidation and coupled hydrogen generation

Daniel Martín-Yerga[a#*], Xiaowen Yu[b], Irina Terekhina[b], Gunnar Henriksson[c], Ann Cornell[a*]

[a]Department of Chemical Engineering, KTH Royal Institute of Technology, SE-100 44 Stockholm, Sweden

[b]Department of Materials and Environmental Chemistry, Stockholm University, SE-106 91 Stockholm, Sweden

[c]Department of Fibre and Polymer Technology, KTH Royal Institute of Technology, SE-100 44 Stockholm, Sweden

[#] Current address:

Department of Chemistry, University of Warwick, Coventry CV4 7AL, United Kingdom

*Corresponding authors e-mails:

(D. M-Y) daniel.martin-yerga@warwick.ac.uk

(A. C) amco@kth.se

EXPERIMENTAL

Solutions and reagents

Nickel(II) nitrate hexahydrate, palladium(II) chloride (> 59.0% Pd; >99.9%, metal basis), sodium chloride, sodium hydroxide, sulfuric acid (HPLC grade), lactic acid (90% solution), ethanol (absolute grade) and pyruvic acid were purchased from VWR (Radnor, PA, USA). Hydrochloric acid (37%) was purchased from Sigma-Aldrich (St. Louis, MO, USA). Nickel foam (1.6 mm thickness) was purchased from GoodFellow (Huntingdon, UK). All reagents were at least of analytical grade. Ultrapure water obtained with a Millipore DirectQ3 purification system from Millipore (Burlignton, MA, USA) was used throughout this work. The electrodeposition solution was composed of 100 mM $Ni(NO_3)_2$ and 1.5 mM $PdCl_2$ in 0.3 M HCl and 0.5 M NaCl. All the experiments with lactic and pyruvic acids were performed in NaOH solution with ultrapure water and were prepared daily before the experiments. Alkaline media was used since Ni (used as electrode material) is not stable in acidic conditions, particularly at anodic potentials. NaOH concentration was higher or equal to lactic acid concentration in order to ensure alkaline conditions, and therefore, lactic acid was in lactate form.

Electrocatalyst preparation

PdNi catalysts were prepared onto Ni foam pieces (1.5 x 1.0 cm) by galvanostatic electrodeposition (-50 mA, 60 s) using a two-electrode cell with a carbon rod counter electrode. Ni foam pieces were cleaned before the electrodeposition by ultrasonication in acetone (10 min) to remove adsorbed organic substances and in aqueous HCl solution (~6 M) to remove oxide layers followed by thoroughly rinsing with ultrapure water.

Electrochemical measurements

Electrochemical measurements were performed using a PAR273A potentiostat/galvanostat from Ametek (Minneapolis, MN, USA). Electrochemical measurements were conducted in a 100 mL glass three-electrode cell with a Pt mesh counter electrode and a Hg/HgO reference electrode (RE-A6P, Bio-Logic, 1 M NaOH). Current densities are presented considering the geometric area of the Ni foam substrate (3 cm^2). All measurements were performed at room temperature (20 ± 2 °C). For product analysis experiments, a 25 mL cell was employed and the counter electrode was separated from the anodic compartment to avoid possible reduction of generated products.

Catalyst physical characterization

Scanning electron microscopy (SEM) was employed to obtain information about the morphology of the $PdNi/Ni_{foam}$ catalyst. A JEOL JSM-7000F instrument was used at an acceleration voltage of 15 kV with a secondary electron detector. Ni_{foam} and $PdNi/Ni_{foam}$ were directly imaged without any preparation. The elemental identification and elucidation of Pd:Ni atomic ratio was carried out by Energy-dispersive X-ray spectroscopy (EDX) using the integrated detector of the SEM instrument. In order to avoid the

effect of the Ni foam substrate on the quantification, the samples were previously ultrasonicated in ethanol (for 60 min) to release individual PdNi nanoparticles/aggregates, which were deposited on a glassy carbon substrate for the EDX analysis. Values of Pd:Ni atomic ratio are the average of three different individual PdNi nanoparticles/aggregates.

Transmission electron microscopy (TEM) images were recorded on a JEOL JEM-2100F TEM operated at 200 keV. PdNi nanoparticles were initially removed from the Ni foam substrate by ultrasonication, dispersed in ethanol and dropped on a Cu grid (200 mesh). ImageJ software was used to measure the size of the nanoparticles and calculate the d-spacing values. For the latter, the inverse Fast Fourier Transform (FFT) method was employed.

Product analysis

The volume of H_2 produced during the oxidation of lactic acid was measured using a gas displacement method. The cathodic compartment filled with 1 M NaOH solution was connected by a tube to a graduated cylinder inverted and filled with water, which was displaced when H_2 was produced. Analysis of the oxidation products was carried out by High-Performance Liquid Chromatography (HPLC) on an Agilent 1260 Infinity II system with an Agilent Hi-Plex H column (250 x 4.6 mm) and a refractive index detector (Agilent 1290 Infinity II RID) set on positive polarity. A sample volume of 10 µL was injected onto the column using the autosampler from the instrument. 5 mM HPLC-grade H_2SO_4 was used as eluent at a flowing rate of 0.4 mL min^{-1}. Column and detector temperature were 55 °C. To calculate the product selectivity for pyruvic acid, the number of moles (n) of lactic acid consumed and pyruvic acid produced were obtained by HPLC. Then, the following equation was used to calculate the selectivity considering a 1:1 stoichiometric reaction between lactic acid and pyruvic acid (Figure S8):

$$PA\ selectivity\ (\%) = 100 * \frac{n_{(pyruvic\ acid\ produced)}}{n_{(lactic\ acid\ consumed)}} * \frac{1\ mol_{(lactic\ acid\ consumed)}}{1\ mol_{(pyruvic\ acid\ produced)}}$$

Faradaic efficiency is the yield based on the electrical charge passed during electrolysis. Faraday's laws were used to calculate the Faradaic efficiency of the pyruvic acid production:

$$n = {}^{Q}/_{zF}$$

where n is the number of moles of pyruvic acid produced (determined by HPLC), Q is the total charge passed during the electrolysis, z is the number of electrons transferred in the reaction (2 e^-), and F is the Faraday constant (96485 C mol^{-1}).

ADDITIONAL RESULTS AND DISCUSSION

Physical characterization of the PdNi/Ni_{foam} catalyst

Morphology and compositional characterization of the PdNi catalyst was carried out by Scanning Electron Microscopy (SEM), Energy-dispersive X-ray spectroscopy (EDX) and Transmission Electron Microscopy (TEM).

SEM imaging. Figures S1a-b show the SEM images of the bare Ni foam substrate before (S1a) and after electrodeposition of the PdNi coating (S1b). This coating covered all the surface of the Ni foam substrate demonstrating a good efficiency of the electrodeposition process, but the main 3-dimensional structure of the Ni foam was kept. **Figures S1c-d** show the SEM images at higher magnification where the PdNi coating can be observed in greater detail. In Figure S1d, some of the coating material was slightly scratched partially uncovering the Ni foam substrate. This allowed to obtain some rough estimation of the catalyst thickness, which was measured to be between 1-2 μm. The coating thickness was not fully homogeneous since large particle agglomerates were deposited on several regions (some of them are pointed out by red arrows in the figure). **Figures S1e-f** show SEM images at higher magnification where the nanoscale morphology of the coating is clearly observed. The PdNi layer was formed by heterogeneous nanoparticles (agglomerates) with quite different sizes and a flower-like shape. This particularly interesting structure also suggests a quite rough electrode surface at the nanoscale, which likely contributes to provide a large electrochemical surface area.

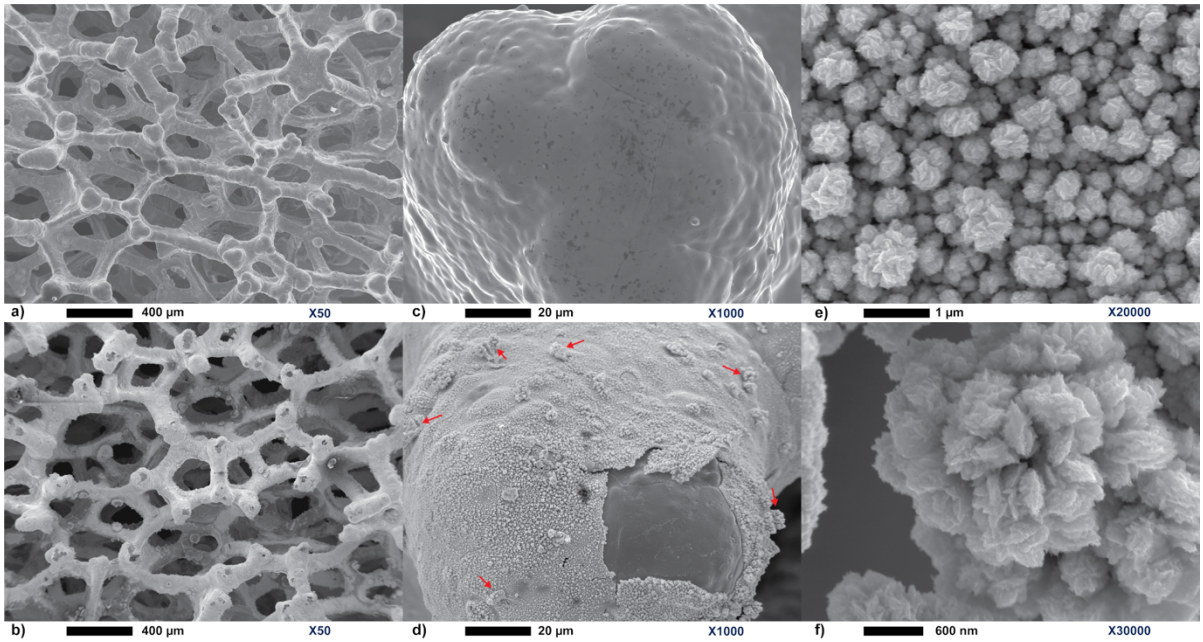

Figure S1. SEM images of the bare Ni_{foam} (a,c) and Ni_{foam} modified with PdNi catalyst (b, d) at X50 and X1000 magnifications, respectively. e, f) SEM images of the PdNi electrodeposited layer at higher magnifications (X20000, X30000) revealing the nanoscale structure of the catalyst.

EDX analysis. To confirm the elemental composition of the coating material, EDX was recorded for individual particles released from the substrate. This was achieved by ultrasonicating the PdNi/Ni_{foam} sample to release the particles of the coated material and avoid the effect of the Ni substrate in the compositional analysis. **Figure S2** shows the SEM image of an individual particle agglomerate (about 200 nm) from the catalyst coating deposited on a glassy carbon substrate, which was further analysed by EDX (**Figure S2b**) confirming that the material was composed by Pd and Ni. Measurements of three different particles led to an average Pd:Ni atomic ratio of 87:13 (±3) for the catalyst.

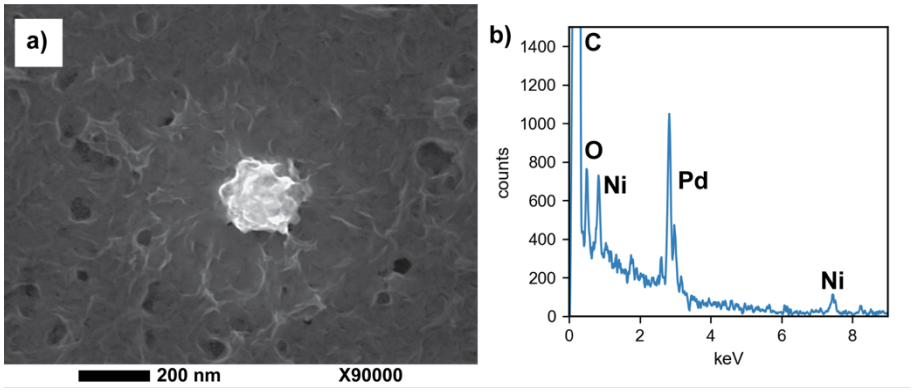

Figure S2. a) SEM image of a single PdNi nanoparticle removed from the substrate by ultrasonication. b) EDX spectrum for the PdNi single particle in a). A high C signal is observed due to the glassy carbon used as support for the measurements.

TEM imaging. To get further information about the properties of the PdNi catalyst, particles/aggregates released after sonication of the PdNi/Ni_{foam} sample were analysed by TEM. TEM images of the PdNi aggregates at different magnifications (**Figure S3**) show that the large particles observed by SEM are mainly formed by aggregation of numerous smaller nanoparticles. The nanoparticles observed by TEM are also quite heterogeneous having sizes ranging from less than 10 nm to a few tens of nm. TEM images (**Figure S4a**) were further analysed to get information about the crystalline structure of the nanoparticles. For instance, **Figure S4b** show the Fast Fourier Transform (FFT) representation of the TEM image in S4a where the polycrystallinity of the sample can be easily discerned. The inverse FFT method was applied to the different diffraction spots to measure the interplanar distances (d spacings) and relate them to the crystalline structure. **Figure S4c** shows some line profiles obtained from the inverse FFT performed after selectively masking specific diffraction spots in the FFT patterns. Interplanar distances of 0.222, 0.197, 0.136 and 0.119 nm were measured for different diffraction spots, which agrees well with those expected for the (111), (200), (220) and (311) lattice planes of the face-centered cubic (fcc) structure of Pd (JCPDS No. 46-1043).[1] Additionally, interplanar distances of 0.239, 0.213 and 0.153 nm were also observed, which can be assigned to the (111), (200) and (220) lattice planes of the NiO fcc

structure (JCPDS No. 47-1049).[2] No interplanar distances expected for lattice planes of metallic Ni foam (JCPDS No. 04-0850)[1,3] were observed, indicating that the NiO phase is likely part of the PdNi coating formed during the electrodeposition and not from the surface of the Ni foam substrate (which should not be present in these samples).

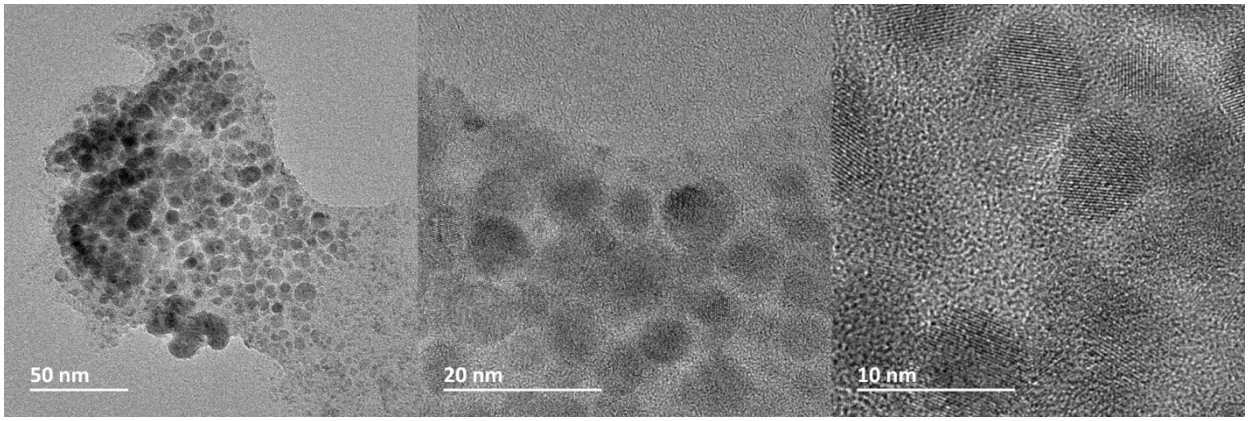

Figure S3. TEM images of the PdNi aggregates at different magnifications.

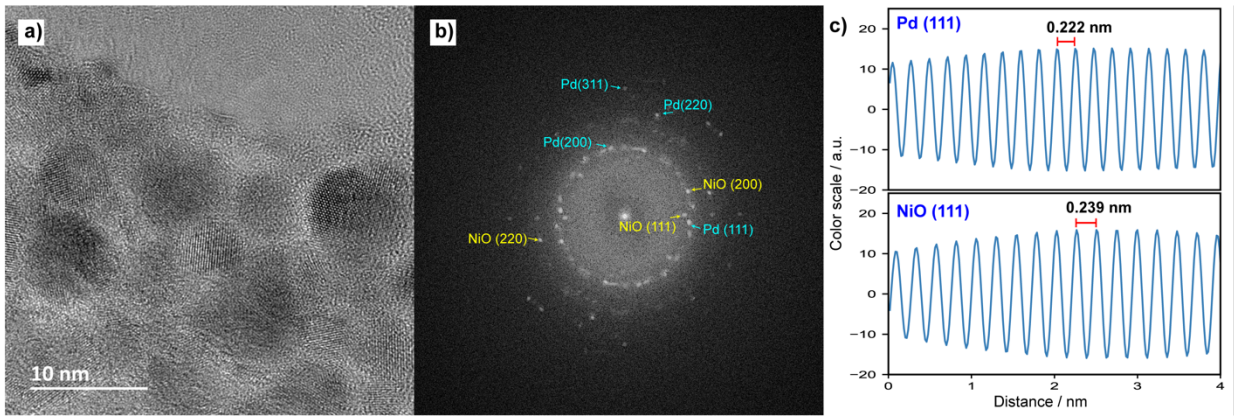

Figure S4. a) TEM image of the PdNi catalyst, which was analyzed to get diffraction information. b) FFT pattern obtained from the same TEM image. c) Line profiles obtained from the inverse FFT performed after selectively masking specific diffraction spots from b.

ADDITIONAL FIGURES

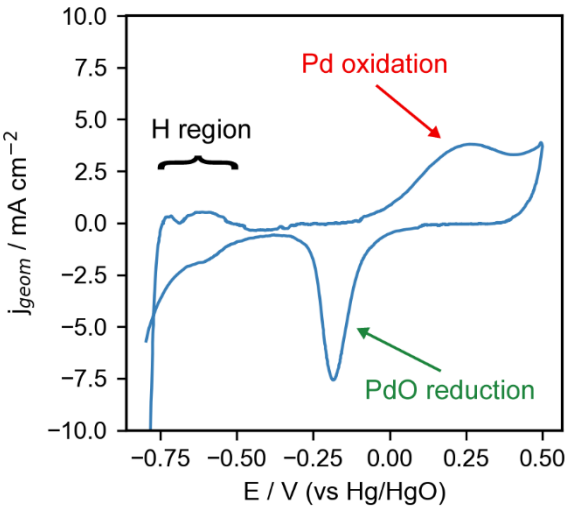

Figure S5. Cyclic voltammetry recorded in 1 M NaOH using the PdNi/Ni_{foam} catalyst, which illustrates the main catalyst surface reactions. Scan rate was 10 mV s^{-1}.

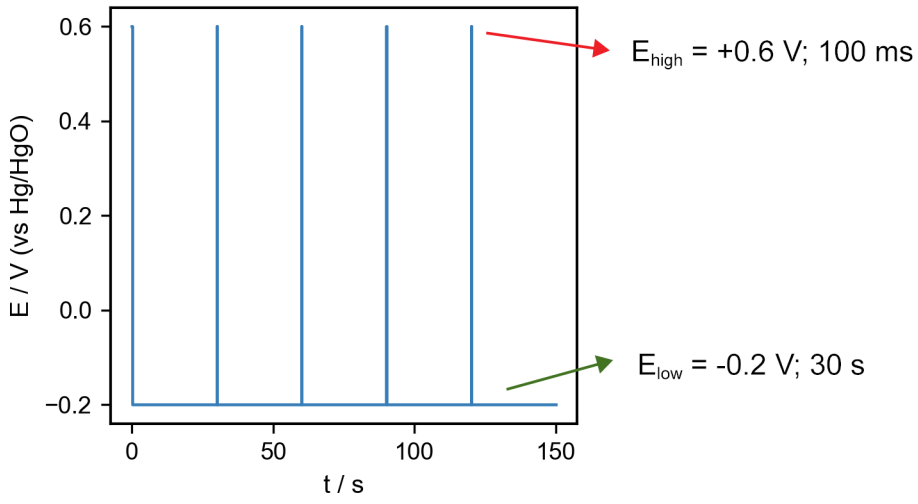

Figure S6. Optimized potential pulsed program to enable the periodic catalyst reactivation, consisting of applying +0.6 V for 100 ms and -0.2 V for 30 s.

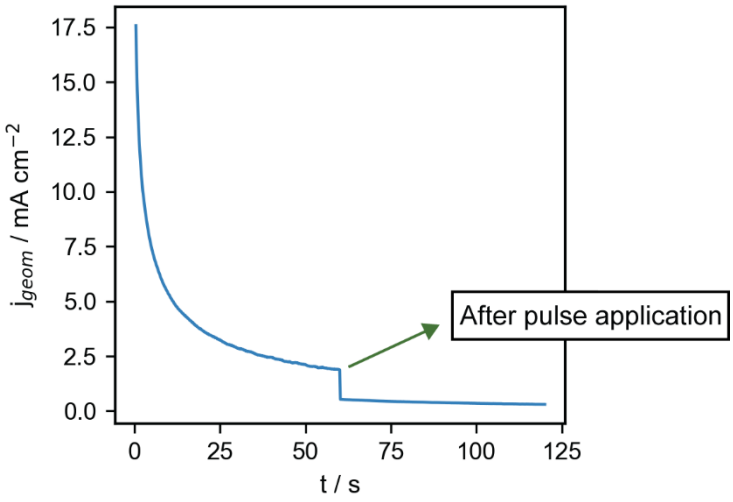

Figure S7. Potentiostatic response obtained for oxidation of 1 M LA in 1 M NaOH using the conventional method (0 V) before and after applying a potential pulse of +0.6 V for 100 ms. Current densities were almost zero after the pulse application as a result of catalyst deactivation and because 0 V is not enough to induce the catalyst reactivation.

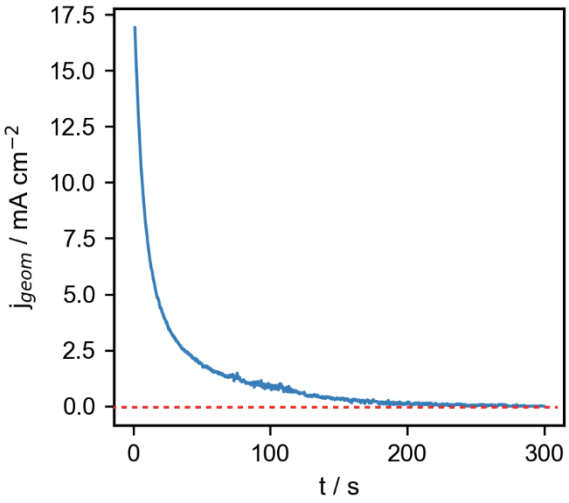

Figure S8. Potentiostatic response obtained for the oxidation of 1 M LA in 1 M NaOH by the conventional method (0 V for 300 s). Current densities were very close to zero after approximately 200 s of the experiment.

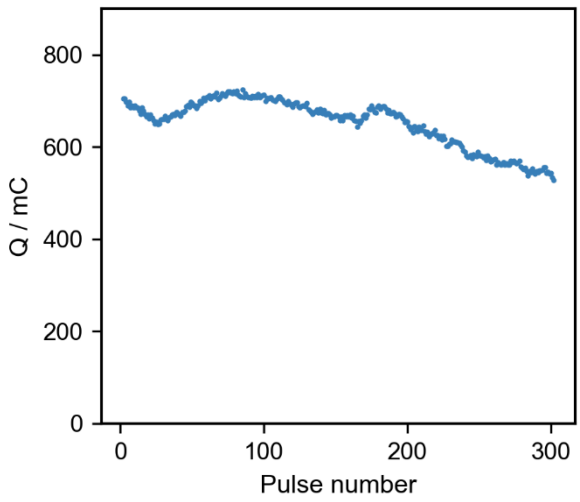

Figure S9. Charge recorded by pulse for the oxidation of 1 M LA in 1 M NaOH by the in situ catalyst reactivation method (0.6 V for 100 ms and -0.2 V for 30 s). This response demonstrates the good stability of the regenerated catalyst surface for longer-term experiments (300 pulses, 2.5 h).

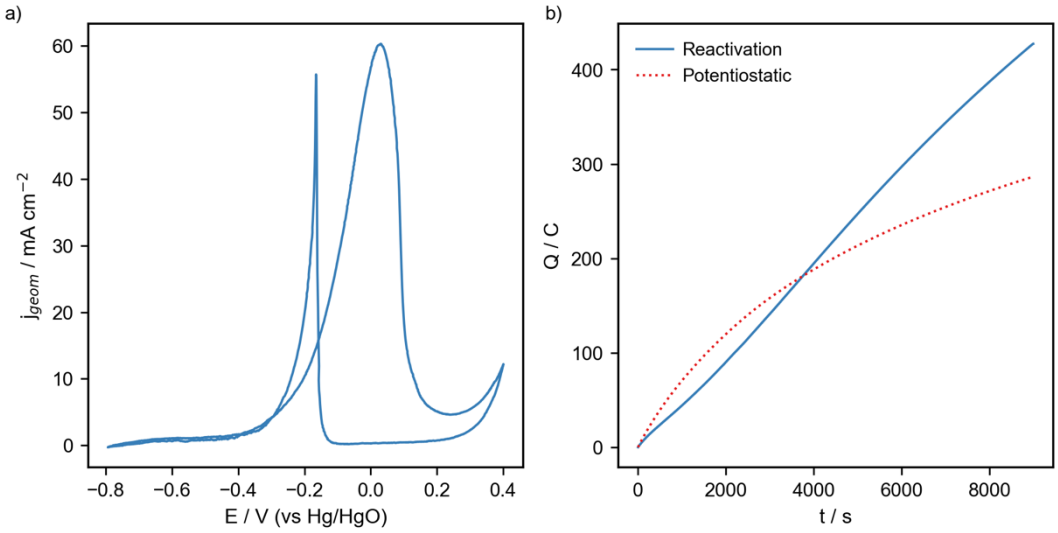

Figure S10. a) Cyclic voltammogram of 1 M Ethanol in 1 M NaOH using the PdNi/Ni_{foam} catalyst. Scan rate was 10 mV/s. b) Accumulated charge recorded for the oxidation of 1 M Ethanol in 1 M NaOH using a potentiostatic method at 0 V (red dashed curve) and the in situ reactivation method (blue curve). The reactivation method was performed applying the optimized pulse program (+0.6 V for 100 ms and -0.20 V for 30 s). The accumulated charge for ethanol oxidation using the regeneration method exceeded that recorded with the potentiostatic method after ~3800 s, demonstrating the benefits of using this method for long-term experiments. For lactic acid oxidation, the advantage of the method was evident at shorter times (see main manuscript) since the j_{pb}/j_{pf} ratio is significantly higher than for ethanol oxidation under the experimental conditions.

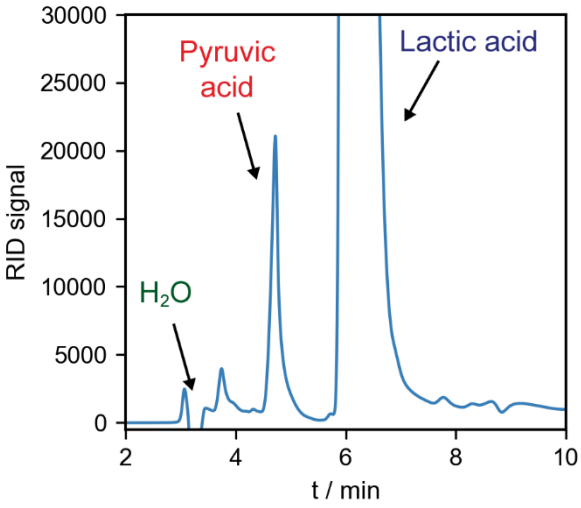

Figure S11. Typical HPLC chromatogram obtained for the oxidation of 1 M LA in 1 M NaOH using the in situ reactivation method (480 pulses, 4 h). Main product detected was pyruvic acid.

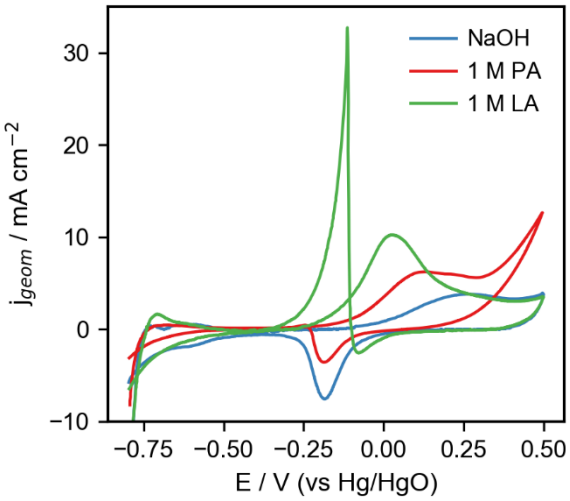

Figure S12. Cyclic voltammograms obtained for the oxidation of 1 M LA or 1 M PA in 1 M NaOH at 10 mV s^{-1}. A higher current density was observed for the PA oxidation (red curve) at around 0 V compared to the blank response (blue curve), but lower than that recorded for LA oxidation. Interestingly, an increased current density was observed at potentials above +0.40 V, suggesting that a more positive potential is required for significant PA oxidation. In addition, the sharp reactivation anodic peak was not observed for PA oxidation during the backward sweep.

REFERENCES

1 X. Niu, H. Zhao and M. Lan, *Journal of Power Sources*, 2016, **306**, 361–368.
2 D. Su, M. Ford and G. Wang, *Sci Rep*, 2012, **2**, 924.
3 M. K. Singh, A. Agarwal, R. Gopal, R. K. Swarnkar and R. K. Kotnala, *J. Mater. Chem.*, 2011, **21**, 11074–11079.